Gene 774 (2021) 145430

Contents lists available at ScienceDirect

Gene

journal homepage: www.elsevier.com/locate/gene

Research paper

Immunogene expression analysis in betanodavirus infected-Senegalese sole using an OpenArray® platform

Juan Gémez-Mata [a,1], Alejandro M. Labella [a,1], Isabel Bandín [b], Juan J. Borrego [a], Esther García-Rosado [a,*]

[a] Universidad de Málaga, Instituto de Biotecnología y Desarrollo Azul, IBYDA, Departamento de Microbiología, Facultad de Ciencias, Málaga, Spain
[b] Universidade de Santiago de Compostela, Instituto de Acuicultura, Departamento de Microbiología y Parasitología, Santiago de Compostela, Spain

ARTICLE INFO

Keywords:
Solea senegalensis
Reassortant nervous necrosis virus
Immune response
OpenArray®
Differentially expressed genes (DEGs)

ABSTRACT

The transcriptomic response of Senegalese sole (*Solea senegalensis*) triggered by two betanodaviruses with different virulence to that fish species has been assessed using an OpenArray® platform based on TaqMan™ quantitative PCR. The transcription of 112 genes per sample has been evaluated at two sampling times in two organs (head kidney and eye/brain-pooled samples). Those genes were involved in several roles or pathways, such as viral recognition, regulation of type I (IFN-1)-dependent immune responses, JAK-STAT cascade, interferon stimulated genes, protein ubiquitination, virus responsive genes, complement system, inflammatory response, other immune system effectors, regulation of T-cell proliferation, and proteolysis and apoptosis. The highly virulent isolate, wSs160.3, a wild type reassortant containing a RGNNV-type RNA1 and a SJNNV-type RNA2 segments, induced the expression of a higher number of genes in both tested organs than the moderately virulent strain, a recombinant harbouring mutations in the protruding domain of the capsid protein. The number of differentially expressed genes was higher 2 days after the infection with the wild type isolate than at 3 days post-inoculation. The wild type isolate also elicited an exacerbated interferon 1 response, which, instead of

Abbreviations: MDA5, Melanoma differentiation-associated gene 5; DHX58, DExH-box helicase 58; PARP12, Poly(ADP-Ribose) polymerase family member 12; TLR, Toll-like receptor; MYD88, Myeloid differentiation primary response; TRAF3, *TNF receptor associated factor 3*; TBKBP1, TBK binding protein; TANK, TRAF family member associated NFKB activator; IRF, Interferon regulatory factor; STAT1, Signal transducer and activator of transcription; SOCS1, Suppressor of cytokine signaling 1; IFN, Interferon; IFNAR1, Interferon alpha and beta receptor subunit 1; ISG, Interferon stimulated gene; IL10RB, Interleukin 10 receptor subunit beta; GIG1, Gigas 1 gene; IFIT1, *Interferon 1-induced proteins t*etratricopeptide repeats; IFI44, *Interferon induced protein 44*; VLIG, Very large inducible GTPase proteins; Mx, Myxovirus resistance protein; PKR, Protein kinase RNA-activated; HERC, E3 Ubiquitin-*protein* ligase; MAGEL2, Melanoma-associated antigen-like protein 2; USP18, Ubiquitin specific peptidase 18; GILT, Gamma-interferon-responsive lysosomal thiol protein; UBE1, Ubiquitin activating enzyme E1; MHC_CLASS_II, Major histocompatibility complex class II; RNF213_ALPHA-LIKE, RING-type E3 utiquitin transferase 213; CD20, Cluster of differentiation 20; LLEC2, Lily-type lectin 2; LMAN1, Lectin mannose-binding 1; LGALS9, Galectin 9; LGALS3BP, Galectin-3-binding protein; TRYPAN-PARP-MDP, Trypan-poly (ADP-ribose) polymerase-multi domain protein; RTP3, Receptor-transporting protein 3; SACS, Sacsin-like; TRIM, Tripartite motif-containing protein; NFKB1, Nuclear factor kappa B subunit 1; IGVSET, Immunoglobulin V-type-set; VHSV-IP, Viral hemorrhagic septicemic virus-induced protein; HERPES-GP2-MDP-H, Herpes gp2 multi-domain protein; LITAF, Lipopolysaccharide induced TNF Factor; ZF-A89, Claudin-like zinc-finger protein; ZF-C3H7A, Zinc-finger double-stranded RNA-binding; NANS, Sialic acid synthase; MAPKBP1, Mitogen-Activated Protein Kinase Binding Protein 1; MOS, Proto-oncogene serine/threonine-protein kinase; CCL-C5A, Chemokine CCL-C5a precursor; CCL19L1, C-C motif chemokine ligand 19; CXCL14, C-X-C motif chemokine 14; CCL4, CC chemokine CK3; CXCL25, C-X-C motif chemokine 25; CCK, Cholecystokinin; CCL28, C-C motif chemokine 28; IL17RC, interleukin 17 receptor C; C3, Complement 3; C9, Complement 9; EBI3, Interleukin-27 subunit beta precursor; U-PAR-LY-6-D, u-PAR/Ly-6 domain; SLC3A2, 4F2 cell-surface antigen heavy chain-like; CFHR3, Complement factor H precursor; ENDOG, Endonuclease G; MPEG1, Macrophage-expressed gene 1 protein; ZNFX1, NFX1-type zinc finger-containing protein 1; CTSS, Cathepsin S; CTSL1, Cathepsin L 1; CTSZ, Cathepsin Z; CYBA, Cytochrome b-245 alpha polypeptide; U-PAR, Urokinase plasminogen activator surface receptor; CD200, OX-2 membrane glycoprotein; MCAM, Melanoma cell adhesion molecule; PSCA, Prostate stem cell antigen precursor; ISP2, Inner membrane complex sub-compartment protein 2; TIMD4, T-cell immunoglobulin and mucin domain-containing protein 4; EOMES, Eomesodermin; BIRC5, Baculoviral IAP Repeat Containing 5; DAPL1, Death Associated Protein Like 1; ARHGAP11A, rho GTPase-activating protein 11A; GIMAP8, GTPase IMAP family member 8; ETS1, V-ets erythroblastosis virus E26 oncogene homolog; GSN, Gelsolin; BNIP-2, BCL2 Interacting Protein 2; PKP1, Plakophilin-1; SERPINB1, Leukocyte elastase inhibitor; APOD, Apolipoprotein D; CASP, Caspase; MMP30, Metallopeptidase 30; CD5L, CD5 antigen-like; RPS, 40S ribosomal protein S30.

* Corresponding author.
E-mail address: megarciar@uma.es (E. García-Rosado).
[1] J. Gémez-Mata and A.M. Labella have contributed equally.

https://doi.org/10.1016/j.gene.2021.145430
Received 6 May 2020; Received in revised form 26 November 2020; Accepted 5 January 2021
Available online 11 January 2021

protecting sole against the infection, increases the disease severity by the induction of apoptosis and inflammation-derived immunopathology, although inflammation seems to be modulated by the complement system. Furthermore, results derived from this study suggest a potential important role for some genes with high expression after infection with the highly virulent virus, such as *rtp3*, *sacs* and *isg15*. On the other hand, the infection with the mutant does not induce immune response, probably due to an altered recognition by the host, which is supported by a different viral recognition pathway, involving *myd88* and *tbkbp1*.

1. Introduction

Nervous necrosis virus (NNV) is the causal agent of the viral encephalopathy and retinopathy (VER), or viral nervous necrosis, a disease affecting numerous freshwater and marine fish species, including Senegalese sole (*Solea senegalensis*) (Cutrín et al., 2007; Olveira et al., 2009), which causes vacuolation in central nervous system. NNV belongs to the *Betanodavirus* genus, *Nodaviridae* family; it is a non-enveloped virus, with two single positive sense-RNA segments. RNA1 encodes the RNA-dependent RNA polymerase (RdRp); whereas RNA2 encodes the capsid protein (CP). Besides, NNV transcribes a subgenomic mRNA (RNA3) from the RNA1, encoding two non-structural proteins, B1 and B2 (Sahul Hameed et al., 2019). B1 inhibits apoptosis at early stages of viral replication in order to release new viral particles from the infected cells (Chen et al., 2009), whereas B2 suppresses RNA silencing activity (Iwamoto et al., 2005). According to the sequence of the variable region within the CP gene, NNV has been classified into four genotypes, considered as viral species: striped jack nervous necrosis virus (SJNNV), tiger puffer nervous necrosis virus (TPNNV), red-spotted grouper nervous necrosis virus (RGNNV), and barfin flounder nervous necrosis virus (BFNNV) (Sahul Hameed et al., 2019).

Reassortant isolates, presenting segment combinations of RGNNV and SJNNV genotypes, have been obtained from different fish species. Specifically, Olveira et al. (2009) have isolated a reassortant (wSs160.3) from Senegalese sole harbouring a RGNNV-type RNA1 and a SJNNV-type RNA2 segments (RGNNV/SJNNV reassortant). Compared to the parental isolates, the sequence of this isolate is slightly different. Regarding the CP, the wSs160.3 isolate shows RGNNV-type amino acids at positions 247 and 270 which play an important role in increasing virulence to sole (Labella et al., 2018; Souto et al., 2015b). In fact, Souto et al. (2015b) generated a mutant by reverse genetics (rSs160.03$_{247+270}$) showing SJNNV amino acids at those positions, which causes a reduction of 40% in mortality compared to the mortality caused by the wild type isolate.

In order to determine the role of the immune response in the pathogenesis of betanodaviruses, Labella et al. (2018) applied the RNA-Seq technology to determine differences in the transcriptomic profile of Senegalese sole after infection with these two viruses, the wild type reassortant wSs160.3, highly virulent to sole, and the mutant rSs160.03$_{247+270,}$ moderately virulent. The results showed that a higher number of differently expressed genes (DEGs) was detected after the infection with the highly virulent isolate. These overexpressed genes were mainly related to the immune response and proteolysis, which are probably the most relevant mechanisms involved in the severity of the disease produced by this viral isolate.

Based on the results obtained by this RNA-Seq analysis, in this work a 112-assay system OpenArray® platform (Thermofisher), based on quantitative PCR, has been designed. This platform has been used to determine the time-course of the host immune response in head-kidney and nervous tissues (pools of eye and brain) against infections with the wild type wSs160.3 reassortant and the CP mutant virus (rSs160.03$_{247+270}$).

2. Material and methods

2.1. Viral strains

Two NNV strains were used in this study: wSs160.3, a wild type reassortant containing a RGNNV-type RNA1 and a SJNNV-type RNA2 segments (RGNNV/SJNNV) and highly virulent to Senegalese sole (100% mortality), and a recombinant virus harbouring mutations in the capsid protein, rSs160.03$_{247+270}$, which is moderately virulent to this fish species (Souto et al., 2015b).

Both viral strains were propagated on the E-11 cell line grown in Leibovitz L-15 medium (Gibco) supplemented with 2% foetal bovine serum (FBS) and incubated at 25 °C until cytopathic effects (CPEs) were observed. Viral titration was performed in 96-well plates incubated at 25 °C for 7–10 days. Cells were examined daily for CPE observation, and titres, expressed as $TCID_{50}$/mL, were calculated according to the end-point dilution method (Reed and Muench, 1938).

2.2. Sample processing

Three experimental groups of Senegalese sole specimens (5–10 g) were intramuscularly injected with: (A) L-15 medium, as negative control, (B) wSs160.3 and (C) rSs160.03$_{247+270}$. Both viruses were inoculated at $2x10^5$ $TCID_{50}$/fish (Labella et al., 2018). Animals were euthanized by MS-222 (Sigma-Aldrich) overdose at 2 and 3 days post-inoculation (p.i.), and individual samples of head-kidney and pooled eye/brain from three fish per experimental group were aseptically recovered, immediately frozen in liquid nitrogen, and stored at −80 °C until used.

Fish used in this study have been treated according to the Guidelines of the European Union Council (Directive 2010/63/EU) and the Spanish directive (RD53/2013). To minimize fish suffering, trials were accomplished in accordance to the Bioethics Committee of the UMA (Approved number: 9-2014-A).

2.3. RNA extraction and cDNA synthesis

Samples were homogenized in 1 mL of TRI Reagent (Sigma-Aldrich) using the MM400 (Retsch) homogenizer. A volume of 100 μL of 1-bromo-3-chloropropane (AppliChem) was added, and samples were centrifuged at 12,000 × g at 4 °C for 5 min. The aqueous phase was recovered, and an equal volume of 75% ethanol was added. RNA extraction was carried out using the RNeasy Mini Kit (Qiagen) following manufacturer's instructions. RNA was quantified by spectrophotometry at 260 nm using the NanoDrop system (Thermo Scientific). RNA quality was measured by the absorbance ratios $A_{260/230,}$ between 2.0 and 2.4, and $A_{260/280,}$ between 1.8 and 2.1, as well as by the RNA integrity number (RIN), between 8 and 10.

cDNA was synthetized using MicroAmp Optical 96-well reaction plates (Applied Biosystems) and the High-Capacity cDNA Reverse Transcription Kit (Applied Biosystems). RNA (2 μg) was added to each well containing 2 μL of 10X RT Buffer, 2 μL of 10X RT Random Primers, 1 μL of 25X dNTPs, 1 μL of MultiScribe™ Reverse Transcriptase and 4 μL of RNase-free water. The synthesis profile was 10 min at room temperature, 2 h at 37 °C, 5 min on ice, 10 min at 75 °C and 5 min on ice.

2.4. OpenArray® design and qPCR

For the expression analysis, qPCR reactions based on TaqMan™ probes were performed using a 112 × 24 high-performance OpenArray® chip. The array includes 89 selected genes (expression levels over 1.5 or below −1.5) from the transcriptomic results previously obtained by RNA-Seq (Labella et al., 2018) (Table S1), plus 17 genes which were included based on their important role in fish immune response against viral infections (Table S1), such as viral recognition-related genes (*mda5*, *tlr8*, *myd88*, *traf3*, *tbkbp1* and *tank*); genes involved in type I interferon (IFN-1)-dependent immune response (*infg*, *ifn1*, *ifn2* and *ifnar1*); virus responsive genes (*nfkb1*); genes related to complement system (*c9*) and apoptosis (*endog*, *casp3*, *casp6*, *casp9* and *mmp30*). Three genes have been selected as endogenous according to their stable expression by RNA-Seq (*rps30*, *rps4* and *ubq*) and, finally, three probes complementary to viral segments RNA1 and RNA2 have also been included into the OpenArray® chip. Primers and probes were designed using the Custom TaqMan™ Assay Design Tool with the option TaqMan™ Gene Expression Assays (Life Technologies). Selected transcripts, assay ID, assay sequences, primers and TaqMan™ probes (Reporter dye FAM) and 3' non-fluorescent quencher (NFQ) are indicated in supplementary Table S1.

Quantitative PCRs were performed in the OpenArray® system QuantStudio 12K Flex Real-Time PCR System (Applied System), sited in the Research Central Service of the University of Cordoba (Spain), using the TaqMan™ OpenArray® Real-Time PCR Master Mix kit (Applied Biosystems). Samples were loaded in triplicate into OpenArray® plates.

For gene expression analysis, Ct values were obtained using the Thermo Fisher Connect™ (Thermofisher) online application, and the Relative Quantification (RQ) software. The setup was adjusted with options Benjamini-Hochberg deactivated, maximum Ct was set up at 28, AMP score was activated and HIGHSD was changed to 0.25. Fold change (FC) values were obtained by the $2^{-\Delta\Delta Ct}$ method (Livak and Schmittgen, 2001). Values were normalized with the geometric mean of the endogenous genes *rps4* and *ubq*, which showed a more stable expression by OpenArray®, according to their score values, which were obtained using the Applied Biosystems™ Relative Quantitation Analysis Module (ThermoFisher cloud dashboard), and indicate how the Ct values for an specific endogenous gene varied between samples compared to the other genes used as endogenous. A lower score value means higher gene stability (Table S2). Organs from the negative control group (L-15-injected fish) were used as calibrators. Genes with FC values <-1 (down-regulated) or >1 (up-regulated) and $p < 0.05$ were considered DEGs.

The one-way multivariate analysis of variance (MANOVA) was used to test changes in gene expression after viral challenges. Statistical analyses were performed using SSPS v.26 (SPSS Inc., Chicago, IL, USA), $p < 0.05$ were considered significant.

3. Results and discussion

An OpenArray® system has been used to analyse the Senegalese sole immune response in head-kidney and nervous tissues against infections with two NNV strains, the wild type wSs160.3, a RGNNV/SJNNV reassortant highly virulent to sole (100% mortality), and the CP mutant (rSs160.03$_{247+270}$), which causes a 40% reduction in sole mortality compare to the wild type (Souto et al., 2015b).

The OpenArray® system consists of a large-scale high-performance amplification technique, which is a miniaturization of the TaqMan™ PCR technique, which helps to streamline real-time PCR studies using large numbers of samples, assays, or both. This technique has been used for pathogen detection (Grigorenko et al., 2017), genotyping (El-Hoss et al., 2016) and transcription studies (Patel et al., 2013), including transcriptomic response in fish species under different experimental conditions (Bonacic et al., 2016; Carballo et al., 2017; Hachero-Cruzado et al., 2014; Montero et al., 2015). Using this system, it is possible to analyse numerous samples simultaneously, allowing the use of a high number of biological and technical replicas, which increases the statistical robustness of the results obtained. In addition, the reaction volume is considerably reduced (nanolitres), implying lower cost in reagents and shorter reaction time (Devonshire et al., 2013). Thus, in the present study, 112 × 24 OpenArray® chips have been used (2,688 reactions per chip); furthermore, the QuantStudio 12K Flex Real-Time PCR System can process four chips parallelly, which means a total of 10,752 reactions. In addition, since it is based on cDNA amplification, the OpenArray® system can detect expression of genes that are not observed by RNA-Seq. Thus, the OpenArray® used in the current study has detected significant expression of genes that were not previously detected by RNA-Seq (Labella et al., 2018), such as *mda5*, *myd88*, *tbkbp1*, *ifng*, *c9*, *casp3* and *casp6* (Tables 2 and 3).

3.1. Viral replication and overview of DEGs after infection with both viruses

The wild type virus induced the expression of a higher number of genes in both organs compared to the mutant virus (Table 1). Similar results were described by Labella et al. (2018) by RNA-Seq, identifying a reduction of 37.9% in the number of DEGs detected after the infection with the same mutant. Several authors have described a higher transcriptomic change in fish in response to highly virulent viruses, not only in the course of NNV infections (Moreno et al., 2016), but also in infections produced by viruses belonging to other families, such as reovirus (He et al., 2017), rhabdovirus (Purcell et al., 2004) or birnavirus (Skjesol et al., 2011). Most of these authors related this higher transcriptomic response to higher levels of viral replication of the most virulent viruses. In the present study, replication of both viruses, wild type and CP mutant, was detected in head-kidney (Fig. 1). For both viruses, the pattern of replication was similar, with a significant increase of RNA1 and RNA2 from 2 to 3 days p.i. However, replication of the wild type virus (Fig. 1A) was higher than mutant virus replication (Fig. 1B), or at least quicker, since periods longer that 3 days have not been tested.

The presence of NNV genome and viral infective particles in non-nervous tissues has been previously reported in different fish species (Kim et al., 2018; Souto et al., 2018; Su et al., 2015), being gills, spleen and kidney the non-nervous organs where higher levels of viral RNA have been detected after immersion challenges (Kim et al., 2018). In the present study, viral genome in eye/brain pools was only detected in one fish, and, therefore, it has not been possible to quantify viral replication in these organs. The inability to detect viral genome in nervous tissues at

Table 1
DEGs up- and down-regulated detected by OpenArray® in samples of head-kidney and nervous tissues of Senegalese sole after infection with NNV strains at 2 and 3 days p.i. Percentages are related to the total number of genes included in the array excluding housekeeping and viral genes (106 genes).

	Up-regulated genes (%)	Down-regulated genes (%)	Total DEGs
2 days p.i.			
wSs160.03			
Head-kidney	45 (42.5)	3 (2.8)	48 (45.3)
Eye/Brain	37 (34.9)	1 (0.9)	36 (33.9)
Total	**82**	**4**	**86**
rSs160.03$_{247+270}$			
Head-kidney	4 (3.7)	3 (2.8)	7 (6.6)
Eye/Brain	3 (2.8)	0 (0)	3 (2.8)
Total	**7**	**3**	**10**
3 days p.i.			
wSs160.03			
Head-kidney	9 (8.5)	1 (0.9)	10 (9.4)
Eye/Brain	14 (13.2)	0 (0)	14 (13.2)
Total	**23**	**1**	**24**
rSs160.03$_{247+270}$			
Head-kidney	1 (0.9)	1 (0.9)	2 (1.8)
Eye/Brain	1 (0.9)	0 (0)	1 (0.9)
Total	**2**	**1**	**3**

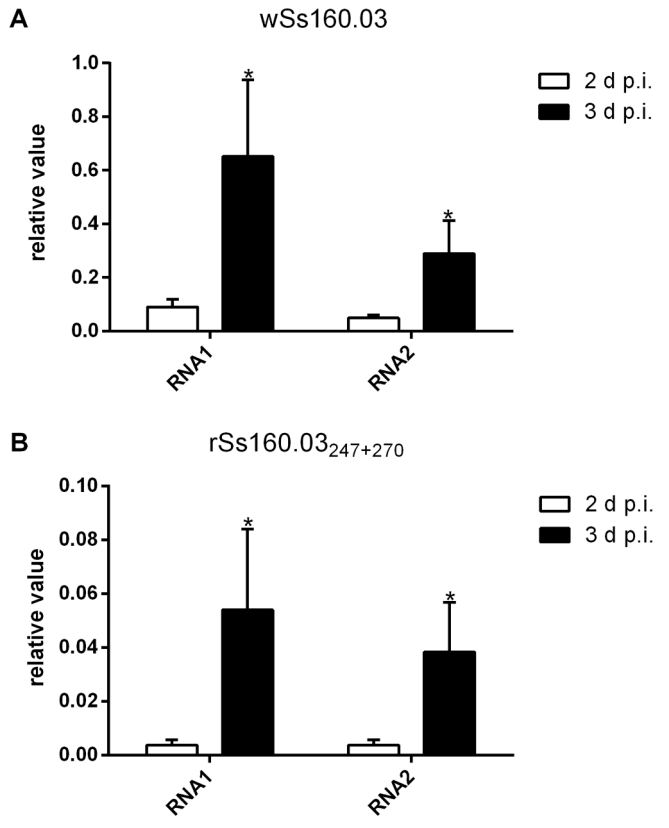

Fig. 1. Relative quantification of wSs160.03 (A) andrSs160.03$_{247+270}$ (B) RNA1 and RNA2 segments in head-kidney at 2 and 3 days post-inoculation. Primers and probes use to amplify each viral segment were included in the OpenArray®chip (Table S1). Results are mean ± standard deviation (SD) (n = 3). Asterisks indicate significant differences throughout time for each RNA segment ($p < 0.05$).

2 and 3 days p.i. could be due to the low level of viral RNA in these tissues at such short times after infection, since viruses firstly spread from the injection site to head-kidney and, afterwards, to the nervous tissues. This hypothesis is supported by the number of induced immunogenes recorded; thus, 45.3% of the analysed genes in head-kidney were induced (45 up-regulated and 3 down-regulated) 2 days after inoculation with the wild type strain, whereas in nervous tissues this virus induces the expression of 33.9% of the analysed genes (37 up-regulated and 1 down-regulated) at the same sampling time (Table 1). However, at 3 days p.i., similarly to the results described by Labella et al. (2018), this proportion has been inverted, and a higher proportion of DEGs has been detected in nervous tissues than in kidney (13.2% and 9.4%, respectively) (Table 1).

Moreover, in this study the number of DEGs after infection with both viruses was higher at 2 days p.i. (when viral RNA level was lower) than at 3 days, meaning that low levels of viral RNA could induce an immune response (Table 1). Specifically, the number of DEGs after infection with the wild type virus was higher than after the infection with the mutant in both organs (86 *vs* 10 at 2 days p.i.; 24 *vs* 3 at 3 days p.i.). Renson et al. (2010) also described a strong and immediate immune response against a highly virulent classical swine fever virus (CSFV) strain, and a progressive and delayed response against a moderately virulent CFSV strain. Therefore, time points longer than 3 days p.i. should be tested in further studies to confirm if a delayed response could be induced by the mutant NNV strain used in the present study.

3.2. Comparative profiling of DEGs in head-kidney and eye/brain pools

Fold change values recorded at different times post-infection in head-kidney and eye/brain pools are shown in Tables 2 and 3, respectively.

The most induced genes after infection with the highly virulent isolate, both in head-kidney and nervous tissue, were those related to the IFN-1 pathway (viral recognition; regulation of IFN-1; JAK-STAT cascade and interferon stimulated genes, ISGs) and virus response genes (VRGs). However, this immune response seems to be ineffective, since, as reported by Souto et al. (2015a), this isolate produces 100% accumulated mortality in Senegalese sole. In this regard, Chaves-Pozo et al. (2019) reported that the immune response triggered by a RGNNV strain in the European sea bass (*Dicentrarchus labrax*) brain-derived cell line (DLB-1) was not potent enough to repeal the infection, since cells finally died. Furthermore, several authors have described that an exacerbate IFN-1 response promotes host susceptibility or disease severity due to the induction of apoptosis, suppression of cell proliferation, and to the inflammation-derived immunopathology (Davidson et al., 2015; Renson et al., 2010).

Hereafter, a detailed exposition and discussion of the most induced DEGs, those related to the IFN-1 pathway and VRGs, is described.

3.2.1. IFN-1 pathway: Viral recognition

Genes related to viral recognition were only expressed 2 days p.i. (Tables 2 and 3). The wild type virus induced the expression of *mda5* in both organs, plus *dhx58* and *tlr3* in head-kidney. All of them were up-regulated, being *dhx58* the gene raising the highest FC level (3.576) (Table 2). On the other hand, the mutant only induced the expression of *myd88* and *tbkbp1* in nervous tissues (Table 3). The expression of different pattern recognition receptors (PRRs) after the infection with both viruses could be a consequence of the mutations displayed by the moderately virulent virus, which are located in the protruding domain of the CP, responsible for virus-cell interaction (Chen et al., 2015; Souto et al., 2015b, 2019). Therefore, the decrease in mortality could be due to an altered recognition of the mutant virus by the sole receptors, as it has been previously suggested by Souto et al. (2015b). PRRs in fish include retinoic acid-inducible gene-I-like receptors (RIG1-like receptors, RLR) and toll-like receptors (TLR) (revised in Langevin et al., 2013). RIG1, melanoma differentiation-associated gene 5 (MDA5) and laboratory of genetics and physiology 2 (LGP2), also known as DHX58, are RLR. Viral genome recognition by RLR induces a signalling pathway involving the TANK-binding kinase 1 (TBK1), which facilitates interferon regulatory factor 3 (IRF3) and IRF7 activation and its translocation into the nucleus for the induction of *ifn1*. TBK1 is also activated by the TBK binding protein (TBKBP1, also known as SINTAD) (Zhu et al., 2019).

On the other hand, TLRs can be involved in the recognition of dsRNAs by TLR3 or 22, or ssRNAs, by TLR7, 8 and 9. TLR7, 8 and 9 adaptor molecule is the myeloid differentiation primary response (Myd88), which is involved in the induction of *ifn1* through NF-κB signalling pathway (Yan et al., 2020). Since the wild type virus mainly induces the expression of *mda5* and *dhx58,* these results suggest that the wild type virus is recognized through RLR in both organs, supporting the idea that levels of MDA5 and DHX58 increase after betanodavirus infection, promoting Mx accumulation (Chen et al., 2014). In contrast, the mutant induces the expression of TLR7, 8 or 9 adaptor (*myd88*) and the *tbkbp1*, an adaptor protein needed for TBK activation (Ryzhakov and Randow, 2007). It has been described that TBKBP1-TBK interaction is not indispensable for IFN-1 induction (Zhu et al., 2019); in fact, in the present study, the overexpression of *tbkbp1* in mutant-injected fish does not produce an IFN-1 response (Tables 2 and 3). Furthermore, zebrafish TBK1-like protein negatively regulates the production of IFN-1 and ISGs (Zhang et al., 2016). Based on these previous reports, the induction of *tbkbp1* recorded in mutant-inoculated fish could account for the lack of expression of ISGs, or even for the down-regulation of *ifit1* and *mx* (Table 2).

3.2.2. IFN-1 pathway: ISGs

Only the inoculation with the highly virulent isolate resulted in the ISG up-regulation in both organs (Tables 2 and 3). In head-kidney, *isg12*,

Table 2
Comparison of gene fold change values in head-kidney after infection with both viruses at different time post-inoculation. Up-regulated genes (fold change >1, $p < 0.05$) are represented in green. Down-regulated genes (fold change <−1, $p < 0.05$) are represented in red. ns: genes not differentially expressed compared to negative control (fold change between −1 and 1) or difference statistically non-significant ($p > 0.05$).

Pathway	Genes	Fold change				p-value			
		Wild type		Mutant		Wild type		Mutant	
		2 d p.i.	3 d p.i.	2 d p.i.	3 d p.i.	2 d p.i.	3 d p.i.	2 d p.i.	3 d p.i.
Viral recognition	*mda5*	1.724	-0.097	0.084	-0.184	5.31e-04	8.43e-01^{ns}	7.18e-01^{ns}	7.51e-01^{ns}
	dhx58	3.576	0.339	-0.175	0.309	4.23e-04	6.99e-01^{ns}	4.38e-01^{ns}	9.04e-01^{ns}
	tlr3	1.608	0.034	-0.361	0.258	2.00e-03	9.63e-01^{ns}	3.40e-01^{ns}	6.63e-01^{ns}
Regulation of type I interferon (IFN)-dependent immune responses	*irf3*	3.320	1.732	0.541	1.107	1.74e-03	1.83e-01^{ns}	2.39e-01^{ns}	4.95e-01^{ns}
	irf7	2.938	0.061	-0.174	2.061	3.83e-03	9.28e-01^{ns}	4.46e-01^{ns}	-
JAK-STAT cascade	*stat1_v1*	2.970	0.791	0.252	0.286	2.74e-02	2.51e-01^{ns}	5.96e-01^{ns}	7.49e-01^{ns}
	stat1_v2	1.395	-0.054	0.331	0.51	3.79e-03	8.66e-01^{ns}	4.51e-01^{ns}	4.21e-01^{ns}
	socs1	2.348	1.019	-0.068	1.659	6.63e-03	-	8.08e-01^{ns}	-
	il10rb	1.836	0.323	-0.303	0.114	5.73e-03	5.26e-01^{ns}	3.73e-01^{ns}	8.40e-01^{ns}
Interferon stimulated genes	*ifng*	1.222	-	-0.646	0.019	3.75e-02	-	3.10e-01^{ns}	9.85e-01^{ns}
	isg15	4.381	3.248	1.119	1.781	5.69e-03	6.78e-02^{ns}	1.64e-01^{ns}	6.52e-01^{ns}
	isg12	2.173	4.320	0.286	3.295	1.86e-02	1.63e-02	6.81e-01^{ns}	5.61e-02^{ns}
	gig1	3.839	3.203	0.186	3.087	4.04e-02	2.54e-02	6.38e-01^{ns}	2.46e-01^{ns}
	ifit1	3.983	2.931	-1.765	2.037	2.88e-03	7.01e-01^{ns}	3.67e-02	2.86e-01^{ns}
	ifi44	2.829	1.958	0.531	0.712	2.46e-03	2.12e-02	2.07e-01^{ns}	4.88e-01^{ns}
	vlig	3.439	-0.164	-1.318	0.28	2.26e-02	-	7.31e-02^{ns}	-
	mx	3.950	1.987	-1.102	0.759	3.48e-02	3.15e-01^{ns}	3.35e-02	6.83e-2^{ns}
	parp12	2.145	0.524	0.257	0.186	2.78e-03	3.52e-01^{ns}	5.09e-01^{ns}	8.43e-01^{ns}
	pkr	1.867	0.196	0.13	0.336	1.55e-03	5.78e-01^{ns}	6.01e-01^{ns}	5.96e-01^{ns}
Protein ubiquitination	*herc4*	4.033	3.048	1.511	1.826	2.07e-03	1.10e-01^{ns}	5.31e-02^{ns}	3.98e-01^{ns}
	herc5	3.585	2.304	0.929	1.197	2.53e-03	9.70e-02^{ns}	6.61e-02^{ns}	4.74e-01^{ns}
	usp18	2.305	1.013	0.162	0.18	5.84e-03	1.65e-01^{ns}	5.51e-01^{ns}	8.63e-2^{ns}
	ube1	2.199	0.752	-0.213	1.448	1.23e-02	-	5.69e-01^{ns}	-
	rnf213_alpha	2.404	1.145	0.071	0.641	1.25e-02	7.96e-02^{ns}	7.74e-01^{ns}	4.21e-01^{ns}
	rnf213_beta	3.003	1.677	0.222	0.582	1.13e-02	1.92e-02	6.47e-01^{ns}	6.48e-01^{ns}
Virus responsive genes	*lman1*	0.499	-2.089	-1.116	-2.054	3.39e-01^{ns}	2.69e-02	4.52e-02	1.74e-02
	lgals3bp	2.531	0.712	0.108	0.589	5.63e-03	3.16e-01^{ns}	3.07e-01^{ns}	5.21e-01^{ns}
	rtp3_v1	5.325	2.67	2.127	1.877	5.20e-03	2.50e-01^{ns}	7.22e-02^{ns}	3.62e-01^{ns}
	rtp3_v2	2.241	1.307	0.682	0.553	1.50e-02	2.91e-01^{ns}	2.40e-01^{ns}	7.72e-01^{ns}
	sacs	4.103	2.234	0.297	0.793	4.26e-03	5.38e-02^{ns}	5.55e-01^{ns}	6.68e-01^{ns}
	trim21	3.315	2.236	1.358	1.409	3.59e-03	9.32e-02^{ns}	6.39e-02^{ns}	3.97e-01^{ns}
	trim39	4.014	2.864	0.119	1.926	2.76e-03	2.05e-02	8.00e-01^{ns}	1.82e-01^{ns}
	igvset	3.173	1.627	0.077	1.196	2.74e-02	1.54e-03	8.60e-01^{ns}	2.39e-01^{ns}
	vhsv-ip	2.642	2.750	0.377	0.766	7.78e-03	4.70e-02	4.37e-01^{ns}	6.45e-01^{ns}
	litaf	1.793	0.595	2.103	-	7.61e-03	5.46e-01^{ns}	7.56e-04	-
Complement	*c3*	-2.695	-1.505	-0.577	-0.297	1.03e-02	2.17e-02^{ns}	7.41e-01^{ns}	7.49e-01^{ns}
	c9	-1.794	-0.759	-0.759	1.057	2.94e-02	-	5.30e-01^{ns}	-
	cfhr3	-2.446	-1.318	-1.501	-1.165	7.24e-03	1.60e-01^{ns}	1.81e-01^{ns}	4.47e-01^{ns}
Inflammatory response	*ccl4*	2.413	0.709	-0.672	2.775	2.34e-02	-	6.68e-02^{ns}	-
	cxcl14	1.6	-1.738	1.675	1.004	1.05e-01^{ns}	-	3.41e-02	-
	cck	2.015	1.19	-0.827	1.485	3.53e-02	9.47e-02^{ns}	1.64e-01^{ns}	8.13e-02^{ns}
	ebi3	2.532	-0.455	-0.552	0.746	1.96e-03	9.79e-02^{ns}	1.43e-01^{ns}	2.51e-01^{ns}
Immune system effectors	*mpeg1*	1.370	0.418	-0.609	1.394	2.30e-03	1.32e-01^{ns}	1.74e-01^{ns}	5.98e-02^{ns}
	zf-c3h7a	1.747	1.121	-0.137	0.794	8.52e-03	5.60e-02^{ns}	5.20e-01^{ns}	2.52e-01^{ns}
	znfx1	4.314	3.558	0.415	2.12	2.97e-03	4.40e-02	1.36e-01^{ns}	3.72e-01^{ns}
	cd200	1.250	1.078	0.135	0.305	3.53e-02	-	8.11e-01^{ns}	6.90e-01^{ns}
Regulation of T-cell proliferation	*timd4*	1.682	1.065	0.252	1.626	2.60e-02	7.47e-02^{ns}	5.56e-01^{ns}	4.09e-02
Proteolysis and apoptosis	*ctsl1*	2.535	1.325	1.991	1.073	6.55e-04	9.16e-03	5.69e-03	1.05e-01^{ns}
	gsn	-0.935	-0.526	1.622	0.685	8.29e-02^{ns}	6.11e-01^{ns}	2.00e-02	5.47e-01^{ns}
	bnip-2	1.780	-0.102	-0.508	-0.359	1.59e-02	9.35e-01^{ns}	4.65e-01^{ns}	6.70e-01^{ns}
	peptidase_c2	1.109	0.782	-1.1	0.722	2.38e-03	2.61e-01^{ns}	1.28e-01^{ns}	3.02e-01^{ns}

Table 3
Comparison of gene fold change values in eye/brain after infection with both viruses at different times post-inoculation. Up-regulated genes (fold change >1, $p < 0.05$) are represented in green. Down-regulated genes (fold change <−1, $p < 0.05$) are represented in red ns: genes not differentially expressed compared to negative control (fold change between −1 and 1) or difference statistically non-significant ($p > 0.05$).

Pathway	Genes	Fold change				*p*-value			
		Wild type		Mutant		Wild type		Mutant	
		2 d p.i.	3 d p.i.	2 d p.i.	3 d p.i.	2 d p.i.	3 d p.i.	2 d p.i.	3 d p.i.
Viral recognition	*mda5*	1.519	0.651	0.948	-	1.12e-02	2.16e-02^{ns}	1.94e-02^{ns}	-
	myd88	-0.743	-	1.266	-	9.76e-02^{ns}	-	2.71e-02	-
	tbkbp1	-0.255	0.074	1.119	1.637	4.87e-01^{ns}	9.22e-01^{ns}	2.17e-02	-
Regulation of type I interferon (IFN)-dependent immune responses	*irf3*	2.360	1.359	-0.036	3.277	1.55e-02	9.82e-04	9.47e-01^{ns}	2.73e-01^{ns}
JAK-STAT cascade	*stat1_v1*	2.332	1.211	1.028	-	9.05e-03	1.53e-2	1.33e-01^{ns}	-
	stat1_v2	1.366	-	0.75	-	3.19e-04	-	8.24e-02^{ns}	-
	il10rb	2.214	1.697	0.619	-	2.48e-02	9.28e-03	3.19e-01^{ns}	-
Interferon stimulated genes	*isg15*	3.266	3.644	0.255	2.927	2.86e-02	8.06e-02^{ns}	7.58e-01^{ns}	-
	isg12	2.168	2.098	1.067	2.486	2.77e-02	1.05e-01^{ns}	4.62e-01^{ns}	8.77e-02^{ns}
	gig1	2.482	2.128	1.58	-	1.08e-02	3.33e-02	1.18e-01^{ns}	-
	ifit1	3.366	2.770	0.209	3.307	1.33e-02	7.02e-03	7.95e-01^{ns}	-
	ifi44	2.264	1.833	-0.101	-	3.16e-02	2.50e-02	8.55e-01^{ns}	-
	vlig	1.776	-	1.397	-	9.02e-03	-	2.66e-01^{ns}	-
	mx	3.219	1.855	0.214	-	1.70e-02	-	7.68e-01^{ns}	-
	parp12	1.792	0.854	0.503	1.665	5.67e-03	8.36e-01^{ns}	1.03e-01^{ns}	1.12e-01^{ns}
	pkr	1.227	0.546	0.455	1.647	2.07e-02	2.03e-01^{ns}	1.69e-01^{ns}	-
Protein ubiquitination	*herc4*	3.784	2.782	0.518	3.104	5.66e-03	2.40e-02	5.14e-01^{ns}	-
	herc5	2.488	1.718	0.189	2.814	1.80e-02	1.25e-01^{ns}	7.97e-01^{ns}	-
	usp18	1.586	0.612	0.59	-	4.01e-02	1.83e-01^{ns}	2.85e-01^{ns}	-
	ube1	0.983	.7.83	1.142	-	1.03e-01^{ns}	-	4.13e-02	-
	rnf213_alpha	1.834	0.98	0.77	1.147	9.79e-03	1.18e-01^{ns}	8.67e-02^{ns}	1.71e-01^{ns}
	rnf213_beta	2.063	1.822	0.145	-	4.23e-02	3.74e-02	6.72e-01^{ns}	-
Antigen processing and presentation	*mhc_class_ii*	1.012	0.429	1.573	0.961	4.19e-02	4.13e-01^{ns}	8.25e-02^{ns}	1.46e-01^{ns}
Virus responsive genes	*llec-2*	2.538	0.725	1.542	2.836	2.61e-02	-	3.76e-01^{ns}	-
	lgals3	2.862	1.337	1.378	1.441	2.20e-02	3.57e-01^{ns}	3.95e-01^{ns}	-
	trypan-parp-mdp	2.713	0.463	1.934	-	3.23e-02	-	2.50e-01^{ns}	-
	rtp3_v2	2.596	1.835	0.47	-	2.64e-02	1.38e-02	4.97e-01^{ns}	-
	sacs	3.090	1.81	0.367	1.565	1.09e-02	1.50e-01^{ns}	5.64e-01^{ns}	8.80e-02^{ns}
	trim21	2.861	1.565	0.239	3.375	1.37e-02	3.34e-02	7.63e-01^{ns}	2.28e-01^{ns}
	trim39	3.076	1.453	1.381	-	1.01e-02	-	5.09e-01^{ns}	-
	igvset	2.021	2.496	0.266	-	2.03e-02	-	-	-
	vhsv-ip	2.283	2.057	2.305	2.305	5.24e-02^{ns}	3.9943-2	-	-
	herpes-gp2-mdp-b	2.683	1.55	0.882	2.302	4.92e-02	3.99e-01^{ns}	6.34e-01^{ns}	1.70e-01^{ns}
	zf-c3h7a	1.423	1.140	0.036	-0.466	1.70e-02	2.97e-02	8.81e-01^{ns}	2.78e-01^{ns}
Immune system effectors	*mpeg1*	1.188	0.849	0.198	2.896	4.91e-02	3.20e-01^{ns}	6.20e-01^{ns}	-
	znfx1	2.910	2.273	0.239	1.974	1.35e-02	1.60e-02	4.50e-01^{ns}	-
	cyba	1.354	1.032	0.455	-	9.68e-03	2.24e-01^{ns}	7.44e-01^{ns}	-
Immunosuppresion and regulation of anti-tumor activity	*mcam*	-1.127	-0.48	1.375	0.385	4.90e-02	1.74e-01^{ns}	6.65e-02^{ns}	1.46e-01^{ns}
Proteolysis and apoptosis	*gimap8_v2*	1.639	1.012	1.08	2.340	2.54e-02	1.33e-01^{ns}	2.49e-01^{ns}	3.86e-02
	ctsl1	1.286	-	0.825	-	2.65e-02	-	1.39e-01^{ns}	-
	pkp1	2.086	1.466	0.372	-	4.44e-02	1.36e-01^{ns}	8.12e-01^{ns}	-
	casp3	1.002	2.299	0.113	-	3.99e-02	-	8.96e-01^{ns}	-
	casp6	-0.686	1.054	0.885	-	3.91e-01^{ns}	2.21e-02	1.11e-02^{ns}	-

gig1 and *ifi44* have been the only genes expressed at both time points assayed, highlighting *isg12* as the only gene with increased expression at 3 days p.i. (4.32 FC value, Table 2), whereas *gig1* transcription slightly decreased, and *ifi44* transcription decreased one order of magnitude (Table 2). Similar results were observed in eye/brain after wild type-virus infection, being *gig1*, *ifit1* and *ifi44* the only genes up-regulated at both time points, although with fold change values reduced at 3 days p.i. (Table 3). The remaining ISGs were up-regulated in both organs 2 days after inoculation with the wild type virus, being *isg15*, *ifit1* and *mx* the ISGs with the highest expression, which was in head-kidney for *isg15* (4.381; Table 2) , and in eye/brain for *ifit1* (3.366; Table 3). It should be underlined that *ifit1* and *mx* were down-regulated in head-kidney after the infection with the mutant at 2 days p.i. (fold changes: −1.765 and −1.102, respectively). As it has been suggested above, this down-regulation could be a consequence of the overexpression of *tbkbp1*, which negatively regulates the expression of IFN and ISGs in zebrafish (Zhu et al., 2019).

The *isg15* and *mx* genes are two of the most studied ISGs in fish, being both up-regulated in several fish species after poly I:C injection or viral infections (Álvarez-Torres et al., 2017, 2018; García-Rosado et al., 2013; Lin et al., 2015; Moreno et al., 2016; Seppola et al., 2007; Yasuike et al., 2011). An inverse relationship between virulence and stimulation of the IFN-1 system has been previously suggested (Cano et al., 2016; Carballo et al., 2016); however, similarly to the results obtained in the present study, higher levels of expression of *isg15* and *mx* have been induced after the infection with a highly virulent NNV strain in sea bass (Moreno et al., 2018, 2019). Tanaka et al. (1998) describe that IFNs have double function in order to limit the spreading of virus, on one hand they elicit an antiviral state in uninfected cells, and, on the other hand, they promote apoptosis in infected cells. The latest function supports the idea previously exposed that an exacerbate IFN-1 response could be deleterious for the host, inducing apoptosis (Davidson et al., 2015; Renson et al., 2010). In fact, it has been described that several IFN-1 system-related genes, such as IRFs and several ISGs, are pro-apoptotic (Chawla-Sarkar et al., 2003; Heylbroeck et al., 2000; Renson et al., 2010). In the present study, *irf3,* 7, *ifi44* and *pkr* are expressed in both organs after the infection with the wild type virus, which could contribute to apoptosis, the main clinical symptom of the disease, and, therefore, to mortality. However, the implication of IRFs and ISGs in NNV-induced apoptosis has not been described until now; therefore, it would be worthy to investigate this aspect in further studies.

ISG15 is a ubiquitin-like protein that exerts antiviral activity conjugating to cellular or viral proteins through a process called ISGylation (Ritchie and Zhang, 2004), which involved several IFN-1-inducible enzymes, such as E1-activating, E2-conjugating and E3-ligase. HERC5 is an E3-ligase responsible for ISGylation in human cells, whereas HERC6 is the main E3-ligase in mouse cells (revised in Oudshoorn et al., 2012). In the present study, the infection with the highly virulent NNV induces up-regulation of genes involved in protein ubiquitination in both organs, specifically the E3-ligases *herc4* and *herc5* (Tables 2 and 3). Little is known about the function of these enzymes in teleost fish. Specifically, a strong up-regulation of *herc4* has also been described in Atlantic cod (*Gadus morhua*) macrophages treated with poly I:C and in Atlantic salmon (*Salmo salar*) macrophages infected with infectious salmon anaemia virus (ISAV) (Eslamloo et al., 2016; Workenhe et al., 2010); however, Rise et al. (2010) detected down-regulation of *herc4* in asymptomatic betanodavirus Atlantic cod carriers. Therefore, further research is necessary to understand the role of HERC proteins in fish.

3.2.3. Virus responsive genes (VRGs)

Regarding VRGs, only *litaf* was up-regulated after inoculation with both viruses 2 days p.i. in head-kidney, reaching higher values after the inoculation with the mutant strain (2.103) (Table 2). The remaining genes were only up-regulated after the infection with the wild type isolate, most of them at 2 days p.i. It should be noted that the highest expression levels were recorded at 2 days p.i. for *sacs* (4.103 in head-kidney, Table 2 and 3.090 in nervous tissues; Table 3) and for *trim39* (4.014 in head-kidney, Table 2 and 3.076 in nervous tissues; Table 3). Moreover, in head-kidney, one of the two *rtp3* unigenes displayed the highest expression of all the DEGs (5.325; Table 2). Similar results were described by Liu et al. (2016) and Liu et al. (2017) in NNV-inoculated Asian seabass (*Lates calcarifer*), suggesting an important role for RTP3 in the interaction between teleost and betanodavirus. Furthermore, Liu et al. (2017) described a microsatellite in the 3′UTR of *rtp3*, which was associated with resistance of Asian seabass to betanodavirus infection.

Up-regulation of the sacsin-like gene (*sacs*) after viral infections has also been described in other fish species, such as in NNV-infected Atlantic cod (Krasnov et al., 2013; Rise et al., 2010; Tso and Lu, 2018) and in reovirus-infected grass carp (*Ctenopahryn godoidella*) (Dai et al., 2017). In fact, in the latest study, *isg15* and *sacs* were the most expressed genes, similarly to the results recorded in the present study. Sacsins are regulators of the heat shock protein 70 (HSP70) chaperon machinery; therefore, the up-regulation of *sacs* could be a response to the betanodavirus-induced stress (Tso and Lu, 2018). In the present study, expression of HSPs has not been detected; however, other authors have reported the implication of HSPs in betanodavirus infection in several fish species (Chaves-Pozo et al., 2019; Dios et al., 2007; Kim et al., 2017; Liu et al., 2016; Lu et al., 2012).

Regarding TRIM39, it is involved in several biological process in mammals, such as regulation of cellular homeostasis, promotion of apoptosis, regulation of cell cycle progression, and IFN-1-pathway regulation (Huang et al., 2012; Kurata et al., 2013; Roberts et al., 2007; Zhang et al., 2012). In fish, Wang et al. (2016) suggested that TRIM39 exerts an important role in the innate response against viral and bacterial infections. Specifically, grouper (*Epinephelus* spp.) TRIM39 affects the cell cycle progression from G1 to S and inhibits replication of Singapore grouper iridovirus (SGIV) and RGNNV *in vitro*.

It is remarkable how *lman1* is down-regulated in head-kidney after infection with both viruses; being this down-regulation more evident at 3 days p.i. (Table 2). LMAN1, also known as ER-Golgi intermediate compartment 53 kDa protein (ERGIC-53), is an intracellular receptor that facilitates the transport of some glycoprotein, being essential for the formation of infectious arenavirus, coronavirus, and filovirus particles through interaction with their glycoproteins (Klaus et al., 2013). However, NNV are non-enveloped viral particles, and they do not possess glycoproteins; which could be the reason for *lman1* down-regulation.

3.2.4. Complement system and inflammatory response

The expression of *c3, c9* and *cfhr3* (coding for the complement factor H-related protein 3 precursor) was suppressed in head-kidney 2 days after infection with the wild type (Table 2), whereas genes related to the complement system or inflammatory response were not transcribed in nervous tissues. The down-regulation of components of the complement system could be related to an attempt to regulate the inflammatory response during viral infection, as it has been previously suggested for C3 complement in zebrafish (Forn-Cuní et al., 2014). Interestingly, in the present study, it has only been recorded the expression of some chemokines, such as *ccl4*, *cck* and *ebi3,* 2 days after the infection with the wild type virus in head-kidney (Table 2), but the expression of proinflammatory cytokines (*il1b* or *tnfα*) has not been detected. On the other hand, down-regulation of the complement system has also been related to immune evasion mechanisms of some viruses, such as bovine viral diarrhoea virus (BVDV), hepatitis C virus and in the acute stage of a rotavirus infection (Liu et al., 2019; Mawatari et al., 2013). Furthermore, Chinchilla et al. (2015) described that the non-structural protein, NV, of viral haemorrhagic septicaemia virus (VHSV) down-regulates components of the complement. The inhibition of the complement system during betanodavirus infection has not been described to date. Even though NNV does not present any protein which directly interacts with the immune system, this virus evades immune response through the inhibition of apoptosis by B1 protein (Chen et al., 2009), and the suppression of cellular RNA silencing activity by B2 protein (Iwamoto et al.,

2005). Therefore, further research should be performed to discern the role of the complement system during NNV infections, focusing on its role as modulator of the inflammatory response, and/or in the virus ability to counteract the antiviral complement activity.

4. Conclusions

In conclusion, the OpenArray® chip designed in the present study is suitable to detect changes in gene transcription caused by the infections with viruses presenting different levels of virulence. The highly virulent NNV induces a higher and earlier transcriptomic response than the moderately virulent mutant strain, being ISGs and VRGs the most highly expressed genes. This quick and exacerbate response could be responsible for tissue damage due to apoptosis and inflammation, although, at least in the present study, this last immune mechanism can be modulated by the complement system. Therefore, it could be interesting to determine the role of IFN-1-related genes in the development of apoptosis in betanodavirus infections. On the other hand, it would be worthy to investigate the role of the genes showing the highest FC values, *rtp3*, *sacs* and *isg15,* in betanodavirus pathogenesis. Regarding the moderately virulent strain, this virus fails in the induction of the immune response, probably due to an altered recognition by the host, which is supported by the induction of a different viral recognition pathway, involving *myd88* and *tbkbp1*.

CRediT authorship contribution statement

J. Gémez-Mata: Data curation, formal analysis, methodology. A.M. Labella: Methodology, formal analysis, Software, supervision, review and editing. **I. Bandín:** conceptualization, review and editing. **J.J. Borrego:** conceptualization, funding acquisition, review and editing. **E. García-Rosado:** conceptualization, funding acquisition, formal analysis, writing original draft and review.

Declaration of Competing Interest

The authors declare that they have no known competing financial interests or personal relationships that could have appeared to influence the work reported in this paper.

Acknowledgements

This work has been supported by the projects AGL2014-54532-C2 and RTI2018-094687-B-C22 form the Spanish Government (Ministerio de Economía y Competitividad), co-funded by the FEDER.

Appendix A. Supplementary data

Supplementary data to this article can be found online at https://doi.org/10.1016/j.gene.2021.145430.

References

Álvarez-Torres, D., Gómez-Abellán, V., Arizcun, M., García-Rosado, E., Béjar, J., Sepulcre, M.P., 2018. Identification of an interferon-stimulated gene, *isg15*, involved in host immune defense against viral infections in gilthead seabream (*Sparus aurata* L.). Fish Shellfish Immunol. 73, 220–227. https://doi.org/10.1016/j.fsi.2017.12.027.

Álvarez-Torres, D., Podadera, A.M., Alonso, M.C., Bandín, I., Béjar, J., García-Rosado, E., 2017. Molecular characterization and expression analyses of the *Solea senegalensis* interferon-stimulated gene 15 (*isg15*) following NNV infections. Fish Shellfish Immunol. 66, 423–432. https://doi.org/10.1016/j.fsi.2017.05.040.

Bonacic, K., Campoverde, C., Sastre, M., Hachero-Cruzado, I., Ponce, M., Manchado, M., Estevez, A., Gisbert, E., Morais, S., 2016. Mechanisms of lipid metabolism and transport underlying superior performance of Senegalese sole (*Solea senegalensis*, Kaup 1858) larvae fed diets containing n-3 polyunsaturated fatty acids. Aquaculture 450, 383–396. https://doi.org/10.1016/j.aquaculture.2015.07.009.

Cano, I., Collet, B., Pereira, C., Paley, R., van Aerle, R., Stone, D., Taylor, N.G.H., 2016. Erratum: Corrigendum to "*In vivo* virulence of viral haemorrhagic septicaemia virus (VHSV) in rainbow trout *Oncorhynchus mykiss* correlates inversely with *in vitro* Mx gene expression" [Veterinary Microbiology (2016) 187 (31–40)]. Vet. Microbiol. 195, 58–59. https://doi.org/10.1016/j.vetmic.2016.09.002.

Carballo, C., Castro, D., Borrego, J.J., Manchado, M., 2017. Gene expression profiles associated with lymphocystis disease virus (LCDV) in experimentally infected Senegalese sole (*Solea senegalensis*). Fish Shellfish Immunol. 66, 129–139. https://doi.org/10.1016/j.fsi.2017.04.028.

Carballo, C., Garcia-Rosado, E., Borrego, J.J., Alonso, M.C., 2016. SJNNV down-regulates RGNNV replication in European sea bass by the induction of the type I interferon system. Vet. Res. 47, 6. https://doi.org/10.1186/s13567-015-0304-y.

Chaves-Pozo, E., Bandín, I., Olveira, J.G., Esteve-Codina, A., Gómez-Garrido, J., Dabad, M., Alioto, T., Esteban, M.A., Cuesta, A., 2019. European sea bass brain DLB-1 cell line is susceptible to nodavirus: a transcriptomic study. Fish Shellfish Immunol. 86, 14–24. https://doi.org/10.1016/j.fsi.2018.11.024.

Chawla-Sarkar, M., Lindner, D.J., Liu, Y.F., Williams, B.R., Sen, G.C., Silverman, R.H., Borden, E.C., 2003. Apoptosis and interferons: role of interferon-stimulated genes as mediators of apoptosis. Apoptosis 8, 237–249. https://doi.org/10.1023/A:1023668705040.

Chen, L.-J., Su, Y.-C., Hong, J.-R., 2009. Betanodavirus non-structural protein B1: a novel anti-necrotic death factor that modulates cell death in early replication cycle in fish cells. Virology 385 (2), 444–454. https://doi.org/10.1016/j.virol.2008.11.048.

Chen, N.-C., Yoshimura, M., Guan, H.-H., Wang, T.-Y., Misumi, Y., Lin, C.-C., Chuankhayan, P., Nakagawa, A., Chan, S.I., Tsukihara, T., Chen, T.-Y., Chen, C.-J., Fremont, D.H., 2015. Crystal structures of a piscine betanodavirus: mechanisms of capsid assembly and viral infection. PLoS Pathog. 11 (10), e1005203. https://doi.org/10.1371/journal.ppat.100520310.1371/journal.ppat.1005203.g00110.1371/journal.ppat.1005203.g00210.1371/journal.ppat.1005203.g00310.1371/journal.ppat.1005203.g00410.1371/journal.ppat.1005203.g00510.1371/journal.ppat.1005203.t00110.1371/journal.ppat.1005203.s00110.1371/journal.ppat.1005203.s00210.1371/journal.ppat.1005203.s00310.1371/journal.ppat.1005203.s00410.1371/journal.ppat.1005203.s00510.1371/journal.ppat.1005203.s00610.1371/journal.ppat.1005203.s00710.1371/journal.ppat.1005203.s008.

Chen, Y.-M., Wang, T.-Y., Chen, T.-Y., 2014. Immunity to betanodavirus infections of marine fish. Dev. Comp. Immunol. 43, 174–183. https://doi.org/10.1016/j.dci.2013.07.019.

Chinchilla, B., Encinas, P., Estepa, A., Coll, J.M., Gomez-Casado, E., 2015. Transcriptome analysis of rainbow trout in response to non-virion (NV) protein of viral haemorrhagic septicaemia virus (VHSV). Appl. Microbiol. Biotechnol. 99 (4), 1827–1843. https://doi.org/10.1007/s00253-014-6366-3.

Cutrín, J.M., Dopazo, C.P., Thiéry, R., Leao, P., Olveira, J.G., Barja, J.L., Bandín, I., 2007. Emergence of pathogenic betanodaviruses belonging to the SJNNV genogroup in farmed fish species from the Iberian Peninsula. J. Fish Dis. 30 (4), 225–232. https://doi.org/10.1111/jfd.2007.30.issue-410.1111/j.1365-2761.2007.00803.x.

Dai, Z., Li, J., Hu, C., Wang, F., Wang, B., Shi, X., Hou, Q., Huang, W., Lin, G., 2017. Transcriptome data analysis of grass carp (*Ctenopharyngodon idella*) infected by reovirus provides insights into two immune-related genes. Fish Shellfish Immunol. 64, 68–77. https://doi.org/10.1016/j.fsi.2017.03.008.

Davidson, S., Maini, M.K., Wack, A., 2015. Disease-promoting effects of type I interferons in viral, bacterial, and coinfections. J. Interf. Cytokine Res. 35 (4), 252–264. https://doi.org/10.1089/jir.2014.0227.

Devonshire, A.S., Sanders, R., Wilkes, T.M., Taylor, M.S., Foy, C.A., Huggett, J.F., 2013. Application of next generation qPCR and sequencing platforms to mRNA biomarker analysis. Methods 59 (1), 89–100. https://doi.org/10.1016/j.ymeth.2012.07.021.

Dios, S., Poisa-Beiro, L., Figueras, A., Novoa, B., 2007. Suppression subtraction hybridization (SSH) and macroarray techniques reveal differential gene expression profiles in brain of sea bream infected with nodavirus. Mol. Immunol. 44 (9), 2195–2204. https://doi.org/10.1016/j.molimm.2006.11.017.

El-Hoss, J., Jing, D., Evans, K., Toscan, C., Xie, J., Lee, H., Taylor, R.A., Lawrence, M.G., Risbridger, G.P., MacKenzie, K.L., Sutton, R., Lock, R.B., 2016. A single nucleotide polymorphism genotyping platform for the authentication of patient derived xenografts. Oncotarget 7, 60475–60490. https://doi.org/10.18632/oncotarget.11125.

Eslamloo, K., Xue, X., Booman, M., Smith, N.C., Rise, M.L., 2016. Transcriptome profiling of the antiviral immune response in Atlantic cod macrophages. Dev. Comp. Immunol. 63, 187–205. https://doi.org/10.1016/j.dci.2016.05.021.

Forn-Cuní, G., Reis, E.S., Dios, S., Posada, D., Lambris, J.D., Figueras, A., Novoa, B., Foulkes, N.S., 2014. The evolution and appearance of c3 duplications in fish originate an exclusive teleost c3 gene form with anti-inflammatory activity. PLoS One 9 (6), e99673. https://doi.org/10.1371/journal.pone.0099673.

García-Rosado, E., Alonso, M., Fernández-Trujillo, M., Manchado, M., Béjar, J., 2013. Characterization of flatfish Mx proteins. In: Neumann, L., Meier, S. (Eds.), Veterinary Immunology Immunopathololgy. Nova Science Publishers, Inc., New York, pp. 99–129.

Grigorenko, E., Fisher, C., Patel, S., Winkelman, V., Williamsoon, P., Chancey, C., Anez, G., Rios, M., Majam, V., Kumar, S., Ducan, R., 2017. Highly Multiplex Real-Time PCR-based screening for blood-borne pathogens on a OpenArray platform. J. Mol. Diagnost. 19, 549–560. https://doi.org/10.1016/j.jmoldx.2017.03.004.

Hachero-Cruzado, I., Rodríguez-Rua, A., Román-Padilla, J., Ponce, M., Fernández-Díaz, C., Manchado, M., 2014. Characterization of the genomic responses in early Senegalese sole larvae fed diets with different dietary triacylglycerol and total lipids levels. Comp. Biochem. Physiol. - Part D Genom. Proteom. 12, 61–73. https://doi.org/10.1016/j.cbd.2014.09.005.

He, L., Zhang, A., Pei, Y., Chu, P., Li, Y., Huang, R., Liao, L., Zhu, Z., Wang, Y., 2017. Differences in responses of grass carp to different types of grass carp reovirus (GCRV) and the mechanism of hemorrhage revealed by transcriptome sequencing. BMC Genom. 18, 1–15. https://doi.org/10.1186/s12864-017-3824-1.

Heylbroeck, C., Balachandran, S., Servant, M.J., DeLuca, C., Barber, G.N., Lin, R., Hiscott, J., 2000. The IRF-3 transcription factor mediates Sendai Virus-induced apoptosis. J. Virol. 74 (8), 3781–3792. https://doi.org/10.1128/JVI.74.8.3781-3792.2000.

Huang, N.J., Zhang, L., Tang, W., Chen, C., Yang, C.S., Kornbluth, S., 2012. The Trim39 ubiquitin ligase inhibits APC/c cdh1-mediated degradation of the Bax activator MOAP-1. J. Cell Biol. 197, 361–367. https://doi.org/10.1083/jcb.201111141.

Iwamoto, T., Mise, K., Takeda, A., Okinaka, Y., Mori, K.I., Arimoto, M., Okuno, T., Nakai, T., 2005. Characterization of striped jack nervous necrosis virus subgenomic RNA3 and biological activities of its encoded protein B2. J. Gen. Virol. 86, 2807–2816. https://doi.org/10.1099/vir.0.80902-0.

Kim, J.-O., Kim, J.-O., Kim, W.-S., Oh, M.-J., 2017. Characterization of the transcriptome and gene expression of brain tissue in sevenband grouper (*Hyporthodus septemfasciatus*) in response to NNV infection. Genes 8. https://doi.org/10.3390/genes8010031.

Kim, J.-O., Kim, S.-J., Kim, J.-O., Kim, W.-S., Oh, M.-J., 2018. Distribution of nervous necrosis virus (NNV) in infected sevenband grouper, *Hyporthodus septemfasciatus* by intramuscular injecton or immerision challenge. Aquaculture 489, 1–8. https://doi.org/10.1016/j.aquaculture.2018.01.042.

Klaus, J., Eisenhauer, P., Russo, J., Mason, A.B., Do, D., King, B., Taatjes, D., Cornillez-Ty, C., Boyson, J., Thali, M., Zheng, C., Liao, L., Yates, J., Zhang, B., Ballif, B., Botten, J., 2013. The intracellular cargo receptor ERGIC-53 is required for the production of infectious arenavirus, coronavirus and filovirus particles. Cell Host Microbe 14 (5), 522–534. https://doi.org/10.1016/j.chom.2013.10.010.

Krasnov, A., Kileng, Ø., Skugor, S., Jørgensen, S.M., Afanasyev, S., Timmerhaus, G., Sommer, A.-I., Jensen, I., 2013. Genomic analysis of the host response to nervous necrosis virus in Atlantic cod (*Gadus morhua*) brain. Mol. Immunol. 54 (3-4), 443–452. https://doi.org/10.1016/j.molimm.2013.01.010.

Kurata, R., Tajima, A., Yonezawa, T., Inoko, H., 2013. TRIM39R, but not TRIM39B, regulates type I interferon response. Biochem. Biophys. Res. Commun. 436 (1), 90–95. https://doi.org/10.1016/j.bbrc.2013.05.064.

Labella, A.M., Garcia-Rosado, E., Bandín, I., Dopazo, C.P., Castro, D., Alonso, M.C., Borrego, J.J., 2018. Transcriptomic profiles of Senegalese sole infected with nervous necrosis virus reassortants presenting different degree of virulence. Front. Immunol. 9 https://doi.org/10.3389/fimmu.2018.01626.

Langevin, C., Aleksejeva, E., Passoni, G., Palha, N., Levraud, J.-P., Boudinot, P., 2013. The antiviral innate immune response in fish: evolution and conservation of the IFN system. J. Mol. Biol. 425 (24), 4904–4920. https://doi.org/10.1016/j.jmb.2013.09.033.

Lin, J.-Y., Hu, G.-B., Liu, D.-H., Li, S., Liu, Q.-M., Zhang, S.-C., 2015. Molecular cloning and expression analysis of interferon stimulated gene 15 (ISG15) in turbot, *Scophthalmus maximus*. Fish Shellfish Immunol. 45 (2), 895–900. https://doi.org/10.1016/j.fsi.2015.05.050.

Liu, C., Liu, Y., Liang, L., Cui, S., Zhang, Y., 2019. RNA-Seq based transcriptome analysis during bovine viral diarrhoea virus (BVDV) infection. BMC Genom. 20, 1–18. https://doi.org/10.1186/s12864-019-6120-4.

Liu, P., Wang, L., Kwang, J., Yue, G.H., Wong, S.M., 2016. Transcriptome analysis of genes responding to NNV infection in Asian seabass epithelial cells. Fish Shellfish Immunol. 54, 342–352. https://doi.org/10.1016/j.fsi.2016.04.029.

Liu, P., Wang, L., Ye, B.Q., Huang, S., Wong, S.M., Yue, G.H., 2017. Characterization of a novel disease resistance gene *rtp3* and its association with VNN disease resistance in Asian seabass. Fish Shellfish Immunol. 61, 61–67. https://doi.org/10.1016/j.fsi.2016.12.021.

Livak, K., Schmittgen,, 2001. Analysis of relative gene expression data using real-time quantitavie PCR and the $2^{-\Delta\Delta Ct}$ method. Methods 25, 402–408. https://doi.org/10.1006/meth.2001.1262.

Lu, M.-W., Ngou, F.-H., Chao, Y.-M., Lai, Y.-S., Chen, N.-Y., Lee, F.-Y., Chiou, P.P., 2012. Transcriptome characterization and gene expression of *Epinephelus* spp in endoplasmic reticulum stress-related pathway during betanodavirus infection *in vitro*. BMC Genom. 13 (1), 651. https://doi.org/10.1186/1471-2164-13-651.

Mawatari, S., Uto, H., Ido, A., Nakashima, K., Suzuki, T., Kanmura, S., Kumagai, K., Oda, K., Tabu, K., Tamai, T., Moriuchi, A., Oketani, M., Shimada, Y., Sudoh, M., Shoji, I., Tsubouchi, H., 2013. Hepatitis C virus NS3/4A protease inhibits complement activation by cleaving complement component 4. PLoS One 8 (12), e82094. https://doi.org/10.1371/journal.pone.0082094.

Montero, D., Benitez-Dorta, V., Caballero, M.J., Ponce, M., Torrecillas, S., Izquierdo, M., Zamorano, M.J., Manchado, M., 2015. Dietary vegetable oils: Effects on the expression of immune-related genes in Senegalese sole (*Solea senegalensis*) intestine. Fish Shellfish Immunol. 44 (1), 100–108. https://doi.org/10.1016/j.fsi.2015.01.020.

Moreno, P., Garcia-Rosado, E., Borrego, J.J., Alonso, M.C., 2016. Genetic characterization and transcription analyses of the European sea bass (*Dicentrarchus labrax*) *isg15* gene. Fish Shellfish Immunol. 55, 642–646. https://doi.org/10.1016/j.fsi.2016.06.043.

Moreno, P., Lopez-Jimena, B., Randelli, E., Scapigliati, G., Buonocore, F., Garcia-Rosado, E., Borrego, J.J., Alonso, M.C., 2018. Immuno-related gene transcription and antibody response in nodavirus (RGNNV and SJNNV)-infected European sea bass (*Dicentrarchus labrax* L.). Fish Shellfish Immunol. 78, 270–278. https://doi.org/10.1016/j.fsi.2018.04.054.

Moreno, P., Souto, S., Leiva-Rebollo, R., Borrego, J.J., Bandín, I., Alonso, M.C., 2019. Capsid amino acids at positions 247 and 270 are involved in the virulence of betanodaviruses to European sea bass. Sci. Rep. 9, 1–11. https://doi.org/10.1038/s41598-019-50622-1.

Olveira, J.G., Souto, S., Dopazo, C.P., Thiéry, R., Barja, J.L., Bandín, I., 2009. Comparative analysis of both genomic segments of betanodaviruses isolated from epizootic outbreaks in farmed fish species provides evidence for genetic reassortment. J. Gen. Virol. 90, 2940–2951. https://doi.org/10.1099/vir.0.013912-0.

Oudshoorn, D., van Boheemen, S., Sánchez-Aparicio, M.T., Rajsbaum, R., García-Sastre, A., Versteeg, G.A., 2012. HERC6 is the main E3 ligase for global ISG15 conjugation in mouse cells. PLoS One 7 (1), e29870. https://doi.org/10.1371/journal.pone.0029870.

Patel, S.N., Wu, Y., Bao, Y., Mancebo, R., Au-Young, G.E., 2013. TaqMan OpenArray high-throughput transcriptional analysis of human embrionic and induced pluripotent stem cells. In: Lakshmipathy, V., Vemuri, M.C. (Eds.), Pluripotent stem cells, Methods in Molecular Biology (Methods and Protocols). Humana Press, Totowa, NJ. https://doi.org/10.1007/978-1-62703-348-0_15.

Purcell, M.K., Kurath, G., Garver, K.A., Herwig, R.P., Winton, J.R., 2004. Quantitative expression profiling of immune response genes in rainbow trout following infectious haematopoietic necrosis virus (IHNV) infection or DNA vaccination. Fish Shellfish Immunol. 17 (5), 447–462. https://doi.org/10.1016/j.fsi.2004.04.017.

Reed, L.J., Muench, H., 1938. A simple method of estimating fifty per cent endpoints. Am. J. Hyg. 27, 493–497. https://doi.org/10.1093/oxfordjournals.aje.a118408.

Renson, P., Blanchard, Y., Le Dimna, M., Felix, H., Cariolet, R., Jestin, A., Le Potier, M.-F., 2010. Acute induction of cell death-related IFN stimulated genes (ISG) differentiates highly from moderately virulent CSFV strains. Vet. Res. 41 (1), 07. https://doi.org/10.1051/vetres/2009055.

Rise, M.L., Hall, J.R., Rise, M., Hori, T.S., Browne, M.J., Gamperl, A.K., Hubert, S., Kimball, J., Bowman, S., Johnson, S.C., 2010. Impact of asymptomatic nodavirus carrier state and intraperitoneal viral mimic injection on brain transcript expression in Atlantic cod (*Gadus morhua*). Physiol. Genom. 42 (2), 266–280. https://doi.org/10.1152/physiolgenomics.00168.2009.

Ritchie, K.J., Zhang, D.-E., 2004. ISG15: The immunological kin of ubiquitin. Semin. Cell Dev. Biol. 15 (2), 237–246. https://doi.org/10.1016/j.semcdb.2003.12.005.

Roberts, J.D., Chiche, J.D., Kolpa, E.M., Bloch, D.B., Bloch, K.D., 2007. cGMP-dependent protein kinase I interacts with TRIM39R, a novel Rpp21 domain-containing TRIM protein. Am. J. Physiol. – Lung Cell. Mol. Physiol. 293 (4), L903–L912. https://doi.org/10.1152/ajplung.00157.2007.

Ryzhakov, G., Randow, F., 2007. SINTBAD, a novel component of innate antiviral immunity, shares a TBK1-binding domain with NAP1 and TANK. EMBO J. 26 (13), 3180–3190. https://doi.org/10.1038/sj.emboj.7601743.

Sahul Hameed, A.S., Ninawe, A.S., Nakai, T., Chi, S.C., Johnson, K.L., 2019. ICTV virus taxonomy profile: *Nodaviridae*. J. Gen. Virol. 100, 3–4. https://doi.org/10.1099/jgv.0.001170.

Seppola, M., Stenvik, J., Steiro, K., Solstad, T., Robertsen, B., Jensen, I., 2007. Sequence and expression anlysis of an interferon stimulated gene (ISG15) from Atlantic cod (*Gadus morhua* L.). Dev. Comp. Immunol. 31, 156–171. https://doi.org/10.1016/j.dci.2006.05.009.

Skjesol, A., Skjæveland, I., Elnæs, M., Timmerhaus, G., Fredriksen, B.N., Jørgensen, S.M., Krasnov, A., Jørgensen, J.B., 2011. IPNV with high and low virulence: host immune responses and viral mutations during infection. Virol. J. 8 (1), 396. https://doi.org/10.1186/1743-422X-8-396.

Souto, S., Lopez-Jimena, B., Alonso, M.C., García-Rosado, E., Bandín, I., 2015a. Experimental susceptibility of European sea bass and Senegalese sole to different betanodavirus isolates. Vet. Microbiol. 177 (1-2), 53–61. https://doi.org/10.1016/j.vetmic.2015.02.030.

Souto, S., Mérour, E., Biacchesi, S., Brémont, M., Olveira, J.G., Bandín, I., 2015b. *In vitro* and *in vivo* characterization of molecular determinants of virulence in reassortant betanodavirus. J. Gen. Virol. 96, 1287–1296. https://doi.org/10.1099/vir.0.000064.

Souto, S., Olveira, J.G., Alonso, M.C., Dopazo, C.P., Bandín, I., 2018. Betanodavirus infection in bath-challenged *Solea senegalensis* juveniles: a comparative analysis of RGNNV, SJNNV and reassortant strains. J. Fish Dis. 41, 1571–1578. https://doi.org/10.1111/jfd.12865.

Souto, S., Olveira, J.G., García-Rosado, E., Dopazo, C.P., Bandín, I., 2019. Amino acid changes in the capsid protein of a reassortant betanodavirus strain: effect on viral replication *in vitro* and *in vivo*. J. Fish Dis. 42 (2), 221–227. https://doi.org/10.1111/jfd.2019.42.issue-210.1111/jfd.12916.

Su, Y., Xu, H., Ma, H., Feng, J., Wen, W., guo, Z.., 2015. Dynamic distribution and tissue tropism of nervous necrosis virus in juvenile pompano (*Trachinotus ovatus*) during early stages on infection. Aquaculture 440, 25–31. https://doi.org/10.1016/j.aquaculture.2015.01.033.

Tanaka, N., Sato, M., Lamphier, M.S., Nozawa, H., Oda, E., Noguchi, S., Schreiber, R.D., Tsujimoto, Y., Taniguchi, T., 1998. Type I interferons are essential mediators of apoptotic death in virally infected cells. Genes to Cells 3 (1), 29–37. https://doi.org/10.1046/j.1365-2443.1998.00164.x.

Tso, C.-H., Lu, M.-W., 2018. Transcriptome profiling analysis of grouper during nervous necrosis virus persistent infection. Fish Shellfish Immunol. 76, 224–232. https://doi.org/10.1016/j.fsi.2018.03.009.

Wang, W., Huang, Y., Yu, Y., Yang, Y., Xu, M., Chen, X., Ni, S., Qin, Q., Huang, X., 2016. Fish TRIM39 regulates cell cycle progression and exerts its antiviral function against iridovirus and nodavirus. Fish Shellfish Immunol. 50, 1–10. https://doi.org/10.1016/j.fsi.2016.01.016.

Workenhe, S.T., Rise, M.L., Kigenge, M.J.T., Kibenge, F.S.B., 2010. The fight between the teleost fish immune response and aquatic viruses. Mol. Immunol. 47 (16), 2525–2536. https://doi.org/10.1016/j.molimm.2010.06.009.

Yan, X., Zhao, X., Huo, R., Xu, T., 2020. IRF3 and IRF8 regulate NF-κB signaling by targeting MyD88 in teleost fish. Front. Immunol. 11, 1–13. https://doi.org/10.3389/fimmu.2020.00606.

Yasuike, M., Kondo, H., Hirono, I., Aoki, T., 2011. Identification and characterization of Japanese flounder, *Paralichthys olivaceus* interferon-stimulates gene 15 (Jf-ISG15). Comp. Immunol. Microbiol. Infect. Dis. 34, 83–91. https://doi.org/10.1016/j.cimid.2010.02005.

Zhang, L., Chen, W.Q., Hu, Y.W., Wu, X.M., Nie, P., Chang, M.X., 2016. TBK1-like transcript negatively regulates the production of IFN and IFN-stimulated genes through RLRs-MAVS-TBK1 pathway. Fish Shellfish Immunol. 54, 135–143. https://doi.org/10.1016/j.fsi.2016.04.002.

Zhang, L., Mei, Y., Fu, N.-y., Guan, L., Xie, W., Liu, H.-h., Yu, C.-d., Yin, Z., Yu, V.C., You, H., 2012. TRIM39 regulates cell cycle progression and DNA damage responses via stabilizing p21. Proc. Natl. Acad. Sci. USA 109 (51), 20937–20942. https://doi.org/10.1073/pnas.1214156110.

Zhu, L., Li, Y., Xie, X., Zhou, X., Gu, M., Jie, Z., Ko, C.J., Gao, T., Hernandez, B.E., Cheng, X., Sun, S.C., 2019. TBKBP1 and TBK1 form a growth factor signalling axis mediating immunosuppression and tumourigenesis. Nat. Cell Biol. 21 (12), 1604–1614. https://doi.org/10.1038/s41556-019-0429-8.